

Purdue University
Purdue e-Pubs

International Compressor Engineering Conference

School of Mechanical Engineering

1992

Effects of Port Geometry, Dimensions and Position on the Performance of a Rotary Compressor

A. B. Tramschek
University of Strathclyde

K. T. Ooi
Nanyang Technological University

Follow this and additional works at: <https://docs.lib.purdue.edu/icec>

Tramschek, A. B. and Ooi, K. T., "Effects of Port Geometry, Dimensions and Position on the Performance of a Rotary Compressor" (1992). *International Compressor Engineering Conference*. Paper 912.
<https://docs.lib.purdue.edu/icec/912>

This document has been made available through Purdue e-Pubs, a service of the Purdue University Libraries. Please contact epubs@purdue.edu for additional information.

Complete proceedings may be acquired in print and on CD-ROM directly from the Ray W. Herrick Laboratories at <https://engineering.purdue.edu/Herrick/Events/orderlit.html>

EFFECTS OF PORT GEOMETRY, DIMENSIONS AND POSITION ON THE PERFORMANCE OF A ROTARY COMPRESSOR.

Dr A.B. Tramschek,
Senior Lecturer & Dean of Engineering
University of Strathclyde,
Glasgow, Scotland.

Dr K.T. Ooi
School of Mechanical and Production
Engineering,
Nanyang Technological University,
Singapore

ABSTRACT

Rotary sliding vane compressors are positive displacement compressors with built-in volume ratios. Their suction and discharge processes are continuous and thus they are normally valveless machines. The suction and discharge port dimensions and positions thus critically affect the performance of the machine. The paper first presents the effects of the suction port geometry on the performance of the machine. It then follows by examining the influence of both suction and discharge port positions on the machine performance. The analysis was carried out using a theoretical model describing a circular rotor-stator configuration with radially disposed vanes, where the working fluid is air. The resulting effects on the pressure volume diagram and the instantaneous mass-angle of rotation history are shown.

INTRODUCTION

Rotary sliding vane compressors are machines with built-in volume compression ratios. Hence for given machine dimensions, the value of the pressure at the end of the compression process is predetermined by the suction pressure and the actual volume compression ratio. Matching the suction and discharge port positions with the built-in volume ratio is important in order to optimise machine performance. An experimental investigation by Kruse [1] suggested that this matching is the key to improving the machine performance. The analysis that follows examines the effects of suction port geometry and/or port positioning on the machine performance using a theoretical model [2] [3].

PORT DESIGN CONSIDERATIONS

The appropriate choice of the suction and the discharge port positions for compressors with built-in volume ratios depends very much on the variation of the cell volume. Figure 1 shows schematically a typical rotary compressor with eight vanes and table 1 shows its nominal operation conditions and its capacity. The variation of an individual cell volume is shown in Figure 2 from which it may be seen that the maximum cell volume occurs at a leading vane angular position of about 200 degrees whilst the minimum cell volume occurs at 18 degrees. These positions correspond to mid-cell angles of 177.5 degrees and 355.5 degrees respectively. Although a symmetrical rotor-stator arrangement is being considered, deviations of the above angular positions from mid-cell angles of 180 degrees and 360 degrees are caused by the inclusion of the leading vane and its slot as part of the cell volume.

For a correct port design, the maximum cell volume position should correspond to the suction port closing angle whereas the minimum volume position should correspond to the discharge port closing angle. The opening of the suction port is based on the value of the suction pressure. It is best located at the angular position where the cell pressure immediately before the suction port opens is just below the nominal suction pressure. The discharge port opening angle should correspond to the position where the cell pressure reaches a value just above the nominal discharge pressure. The latter position is always delayed for a few degrees if the operational discharge pressure of the compressor is to be varied (especially above the design pressure) as over compression losses are generally smaller than the under-compression losses in terms of their contribution to the indicated power.

EFFECTS OF SUCTION PORT CONFIGURATION

This section discusses the effects of the suction port configuration on the performance of a given compressor. Two different suction port geometries, termed the 'old' port configuration (see Figure 3(a)) and the 'new' port configuration (Figure 3(b)) were investigated, and their influence on the performance of the compressor were compared.

The 'old' suction port (Figure 3(a)) was sited on the end face of the rotor and was located between the crescent shaped gap formed between the rotor and stator. The size of the suction port is thus restricted by the dimensions of the rotor, stator and the offset between the two centres. This particular shape of the suction port produces a particular variation in the port area with respect to the variation of cell volume and influences the breathing characteristic of the compressor. Figure 3(c) shows variation of the active port areas with leading vane angular position. This shape of suction port was found to have certain disadvantages as follows:-

1. The port cross sectional area is small in the region close to the suction port opening position and hence causes a slow recovery in cell pressure during the initial suction stage. This contributes to power losses as may be seen from the pressure volume diagram in Figure 4(e).
2. The maximum width of the suction port area is limited by the dimensions of the rotor, the stator and the offset between their centres.
3. In the simulation study, it was assumed that the cell pressure is uniformly distributed throughout the whole volume of the cell. This assumption may be questionable during the suction process because air needs to flow axially through the end face of the compressor where the suction port is sited and pass along the whole length of the cell before filling the cell volume. During this process some form of axial pressure distribution would be expected and the situation would be exaggerated by a long axial flow path. A simplified simulation of the suction process may be inaccurate.

In an attempt to overcome all these problems a new port configuration was introduced. The change envisaged rectangular-like holes distributed along the stator wall, see Figure 3(b). Predicted results for the two different suction port geometries are shown in Figures 4(a) to 4(f). Figure 4(a) shows the variation of the active suction port area for the old and the new suction ports. It also shows the effects of different axial port length on the variation of the port area for the new port when axial port length varies from 6 mm to 30 mm. It may be seen that the suction port area increases directly as the axial length of the port increases. The extra port area during the initial suction stage causes the cell air mass to increase rapidly (see Figure 4(b)) during the initial suction process. This effect results in rapid pressure recovery as shown in Figure 4(c) and hence improves the breathing characteristics of the compressor as reflected in pressure-volume diagram in Figure 4(e). The resulting variation on cell air temperature is also shown, Figure 4(d). Figures 4(c), 4(e) show that a further reduction in the suction loss is achieved by having a longer axial port length. Figure 4(f) compares the effects of the old and new suction port configuration on the performance of the compressor. Some increase in the free air delivery is achieved by using a new port configuration. The indicated and shaft input power decrease slightly as the axial length of the new port increases and as a result, the specific free air delivery (litre/kWs) increases. However, the benefits diminish when the axial length of the new port exceeded 25 mm. The overall advantages and the improvements stemming from the modified suction port may be summarised as follows:-

- a) The machine shows a better breathing characteristic:- rapid pressure recovery during the suction process. A reduction in the indicated power was predicted.
- b) The size of the suction port is no longer limited by the radii of the rotor and stator as it was before. Speaking in terms of suction port design, this feature provides greater flexibility in the selection of dimensions.

- c) In practice, a shorter flow path for the air induced during the suction process should result in less suction heating and hence improve the volumetric efficiency of a machine. This effects was not included however in the theoretical model.
- d) This port configuration suits better the assumption made in the simulation model that the cell pressure is always distributed uniformly in a cell. Cells may be filled quickly by the air induced because of the axially distributed and shorter flow path.

EFFECTS OF PORT POSITIONING

The effects of the suction and discharge port positions on the pressure volume diagram and the cell air mass versus leading vane angle diagram are illustrated in Figures 5 to 12. Figures 5(a) and 5(b) show the pressure volume diagram and the air mass versus leading vane angle diagram under the correct port positioning. Correct port positioning means that the suction port opens at the position where the cell pressure equals the nominal suction pressure (in reality however, a modest level of partial vacuum must exist inside the cell, to promote air flow into the cell from the suction chamber), the suction port closes as soon as the cell volume attains its maximum value. The discharge port opens as soon as the cell pressure reaches the nominal discharge pressure and closes at the position when the cell volume attains the minimum volume.

In the discussion that follows various symbols are defined:

- P_s : nominal suction pressure
- P_d : nominal discharge pressure
- M_1 : normal residual air mass level before suction process
- M_2 : normal air mass level at the end of suction process

The influence of each port-position is illustrated as follows:-

Suction port opening angle (β)

- a) If the suction port is opened before the cell pressure reaches the nominal suction pressure, under-expansion results. This is illustrated in Figure 6(a). Losses due to this effect are shown by the shaded area in the Figure. The air mass in the cell increases gradually shortly after the commencement of the suction process. See Figure 6(b).
- b) If the port is opened after the cell pressure reaches the nominal suction pressure, over expansion occurs. The cell air mass increases very rapidly in the early stage of the suction process, because of a high pressure differential across the suction port during this period. The effect is shown in Figures 7(a) and 7(b).

Suction port closing angle (β)

- a) If the suction port is closed before the cell volume reaches the maximum cell volume position, a reduction in the cell pressure to a level below that of the nominal suction pressure occurs as the cell volume is still increasing. This premature suction port closing results in a situation where less air is induced into the machine. These effects are illustrated in Figures 8(a) and 8(b). Premature closure of the suction port results in cell pressures less than the nominal discharge pressure when the discharge port opens and backflow occurs through discharge port.
- b) If the suction port is closed after the cell reaches the maximum cell volume position, air inside the cell flows out of the cell through the suction port. This effect is caused by the reduction in the cell volume after the maximum volume position attempting to produce a rise in the cell pressure. This

pressure rise is small and air flows out through the suction port at a constant nominal suction pressure. A delay in port closure results in an under compression condition and may be explained as follows.

consider
$$P_2 = \left(\frac{V_1}{V_2}\right)^n P_1$$

where P_1 is the nominal suction pressure and n is a compression index. As V_1 reduces, and since V_2 is fixed for a given discharge port location the value of P_2 reduces to a value less than the nominal discharge pressure, P_d ; under compression occurs. The effects are shown in Figures 9(a) and 9(b).

Discharge port opening angle (β)

- a) If the discharge port is opened before the pressure in the cell reaches the nominal discharge pressure, under compression results. Reverse flow occurs in the initial stage of the discharge process. This is shown in figures 10(a) and 10(b).
- b) If the discharge port is opened after the cell pressure reaches the nominal discharge pressure, over compression results. Air flows out of the cell during the initial stage of discharge process with a higher velocity than that of the normal condition. This is shown by the steep slope of the cell air mass-angle curve during that period. It is illustrated in Figures 11(a) and 11(b).

Discharge port closing angle (β)

- a) If the discharge port is closed prematurely, more residual air stays in the cell at the end of discharge process. At the same time since the cell volume is still decreasing, the cell pressure rises. Less air will be delivered and less air will be induced following the re-expansion to the suction pressure. This is shown in figures 12(a) and 12(b).
- b) If the discharge port is closed after the cell in question reaches the minimum cell volume position and if the cell is within the sealing arc region then this will not alter either the pressure volume diagram or the cell mass-angle diagram.

CONCLUSION

The effect of the port geometry and port positioning on the performance of a machine is significant. The analysis shows that, to optimise the machine performance, it is important to match the built-in volume ratio with the operational pressure ratio. If a machine has to operate under a wide range of operating pressure ratios, it is suggested that the discharge valve should be used, as mentioned in [1].

NOMENCLATURE

| | |
|------------------------|--|
| FAD (l/s) | Free air delivery |
| P_1 (kW) | Indicated power |
| P_s (kW) | Shaft power |
| R_r (m) | Rotor radius |
| R_s (m) | Stator radius |
| TDC | Top dead centre (angular reference position, 0°) |
| ϵ (mm) | Eccentricity between stator and rotor centres |
| β_1 ($^\circ$) | Suction port opening angle w.r.t. TDC |
| β_2 ($^\circ$) | Suction port closing angle w.r.t. TDC |
| β_3 ($^\circ$) | Discharge port opening angle w.r.t. TDC |
| β_4 ($^\circ$) | Discharge port closing angle w.r.t. TDC |

ACKNOWLEDGEMENT

The authors wish to acknowledge the support received from the Hydrovane Compressor Company Limited during the period of Dr Ooi's doctoral studies.

REFERENCES

1. Kruse, H. "Experimental Investigation on rotary vane compressor." Proceedings of the 1982 Purdue Compressor Technology Conference
2. Tramschek, A.B., Ooi, K.T. "Geometrical optimization of sliding vane compressors." European Conference on Developments in Industrial Compressors, IMechE Headquarters, London Oct. 1989.
3. Ooi, K.T. "Geometrical optimization of rotary sliding vane air compressors." Ph.D Thesis, University of Strathclyde, Glasgow, 1989.

| | | |
|----------------------------|---------------|-------|
| Operating | speed rev/min | 1450 |
| Atmospheric pressure | bar | 1.013 |
| Atmospheric temperature | K | 293 |
| Nominal suction pressure | bar (ABS) | 1.013 |
| Nominal discharge pressure | bar (ABS) | 7.91 |
| Capacity | l/s | 14.9 |

Table 1 Operating conditions and capacity of the compressor

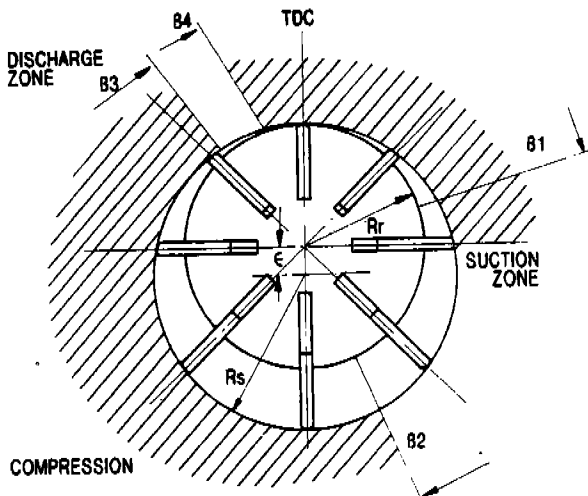


FIGURE 1. SCHEMATIC ARRANGEMENT OF A ROTARY SLIDING VANE COMPRESSOR

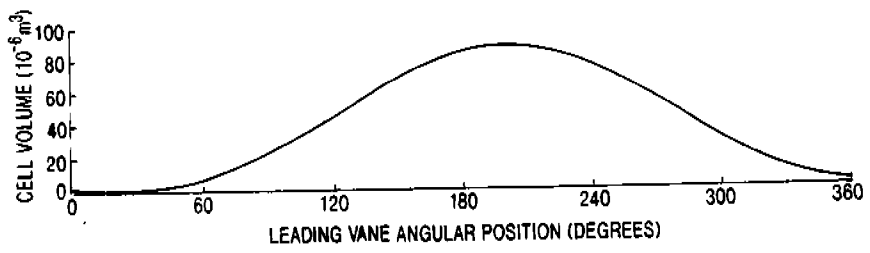


FIGURE 2. VARIATION OF CELL VOLUME.

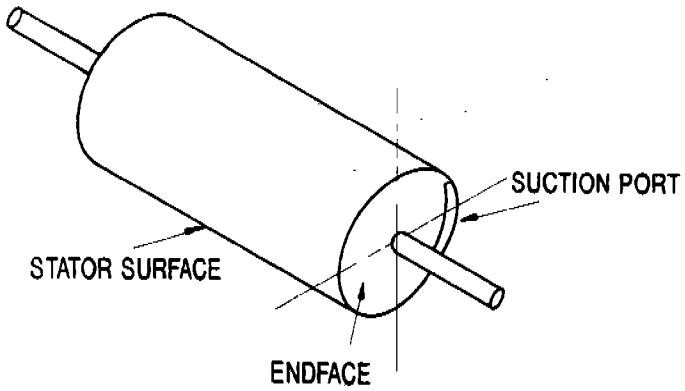


FIGURE 3a 'OLD' SUCTION PORT CONFIGURATION

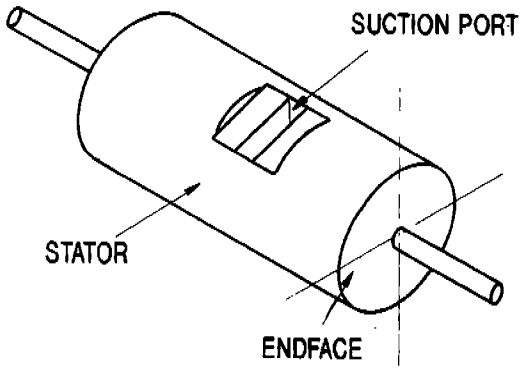


FIGURE 3b 'NEW' SUCTION PORT CONFIGURATION

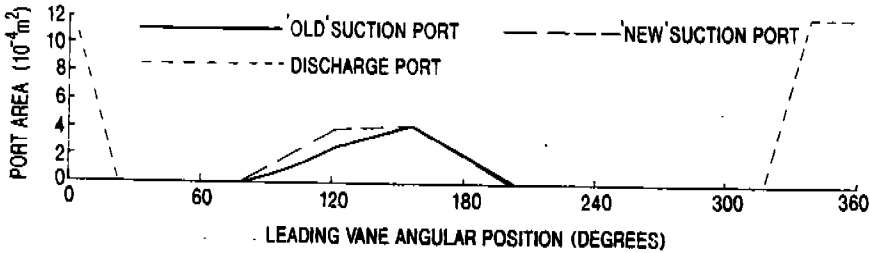


FIGURE 3(c) VARIATION OF ACTIVE PORT

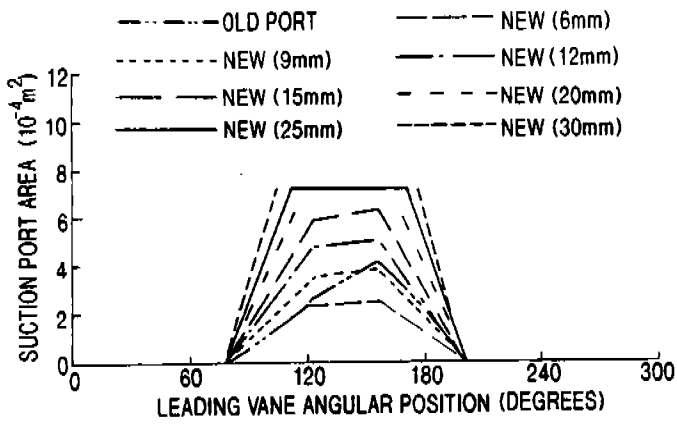


FIGURE 4(a) VARIATION OF ACTIVE SUCTION PORT AREA.

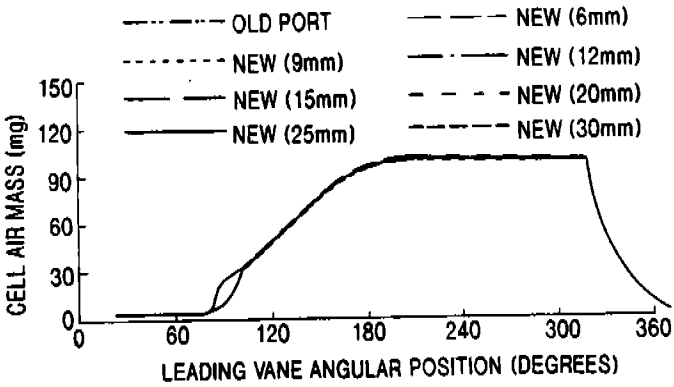


FIGURE 4(b) VARIATION OF CELL AIR MASS

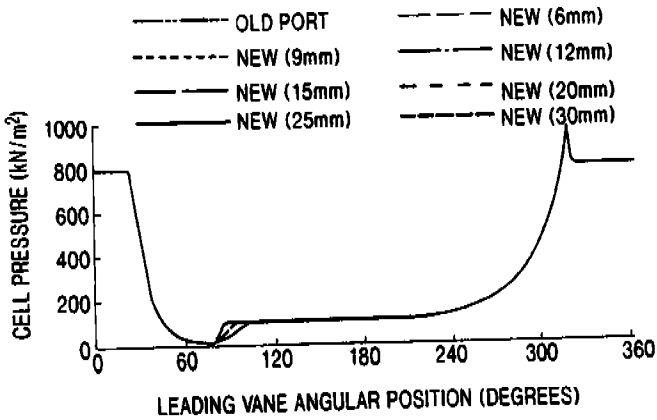


FIGURE 4(c) VARIATION OF CELL PRESSURE

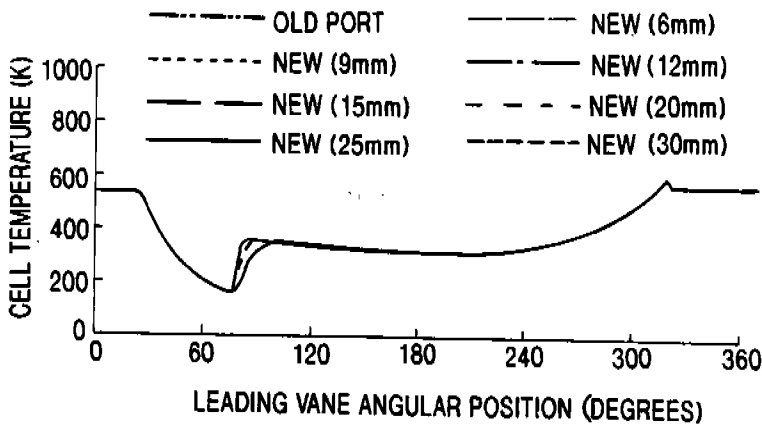


FIGURE 4(d) VARIATION OF CELL TEMPERATURE

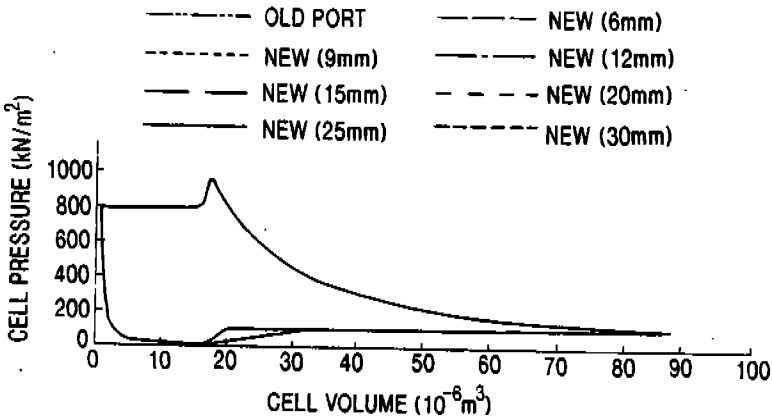


FIGURE 4(e) PRESSURE-VOLUME DIAGRAMS

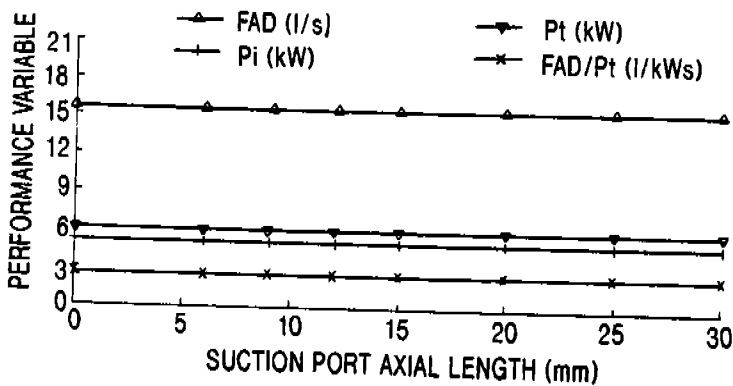


FIGURE 4(f) VARIATION OF COMPRESSOR PERFORMANCE VARIABLE WITH SUCTION PORT AXIAL LENGTH

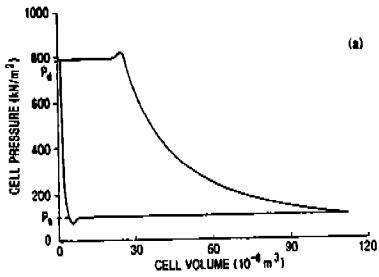


FIGURE 5. P-V DIAGRAM AND CELL AIR MASS-ANGLE DIAGRAM FOR COMPRESSOR OPERATING AT CORRECT PORT POSITIONING

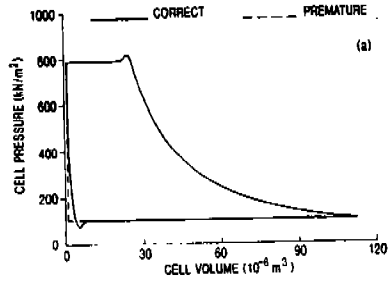
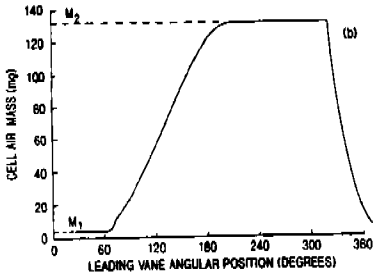


FIGURE 6. P-V DIAGRAM AND CELL AIR MASS-ANGLE DIAGRAM COMPARISON BETWEEN CORRECT AND PREMATURE SUCTION PORT OPENING

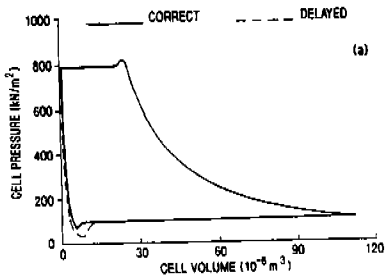
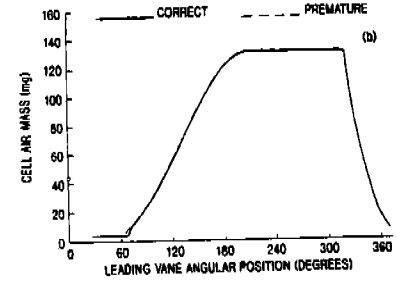


FIGURE 7. P-V DIAGRAM AND CELL AIR MASS-ANGLE DIAGRAM COMPARISON BETWEEN CORRECT AND DELAYED SUCTION PORT OPENING

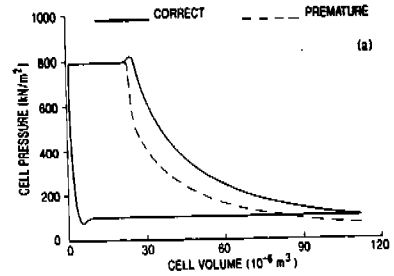
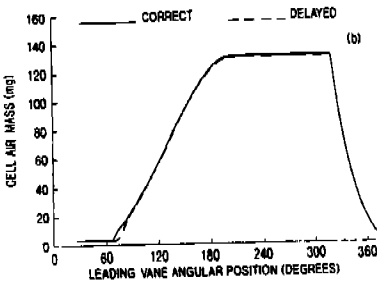
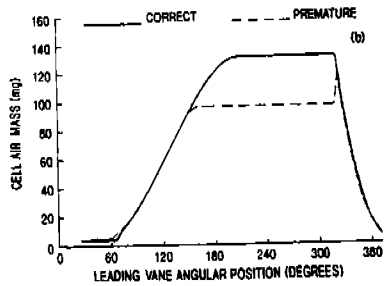


FIGURE 8. P-V DIAGRAM AND CELL AIR MASS-ANGLE DIAGRAM COMPARISON BETWEEN CORRECT AND PREMATURE SUCTION PORT CLOSING



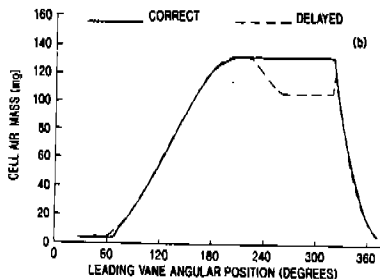
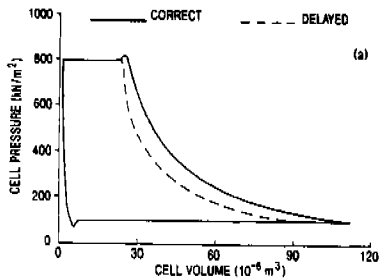


FIGURE 9 P-V DIAGRAM AND CELL AIR MASS-ANGLE DIAGRAM COMPARISON BETWEEN CORRECT AND DELAYED SUCTION PORT CLOSING

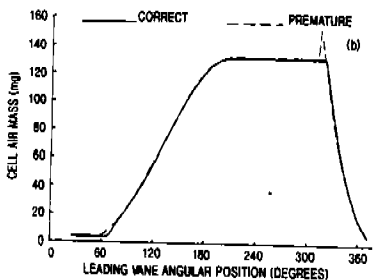
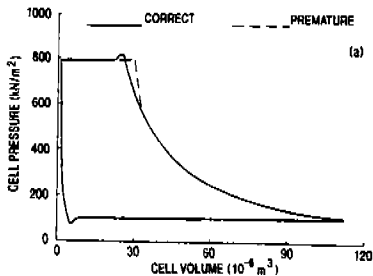


FIGURE 10 P-V DIAGRAM AND CELL AIR MASS-ANGLE DIAGRAM COMPARISON BETWEEN CORRECT AND PREMATURE DISCHARGE PORT OPENING.

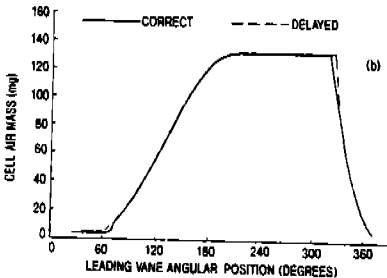
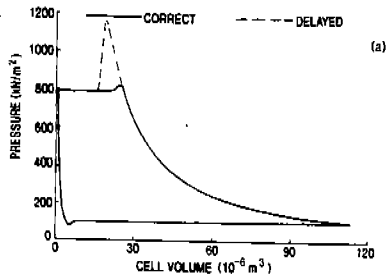


FIGURE 11 P-V DIAGRAM AND CELL AIR MASS-ANGLE DIAGRAM COMPARISON BETWEEN CORRECT AND DELAYED DISCHARGE PORT OPENING.

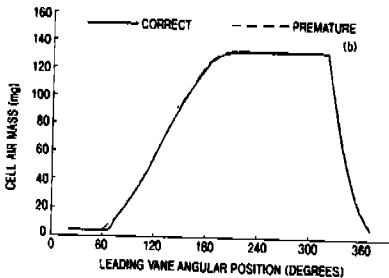
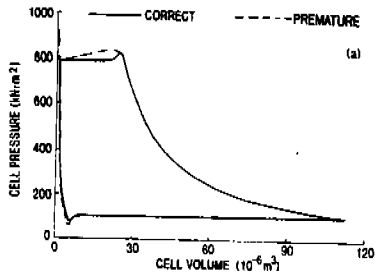


FIGURE 12 P-V DIAGRAM AND CELL AIR MASS-ANGLE DIAGRAM COMPARISON BETWEEN CORRECT AND PREMATURE DISCHARGE PORT CLOSING.